EurJIC

*European Journal of
Inorganic Chemistry*

Accepted Article

FULL PAPER

Addition of Re-Bonded Nucleophilic Ligands to Activated Alkynes: A Theoretical Rationalization

Daniel Álvarez,[a] Jesús Díaz,[b] M. Isabel Menéndez,[a] and Ramón López*[a]

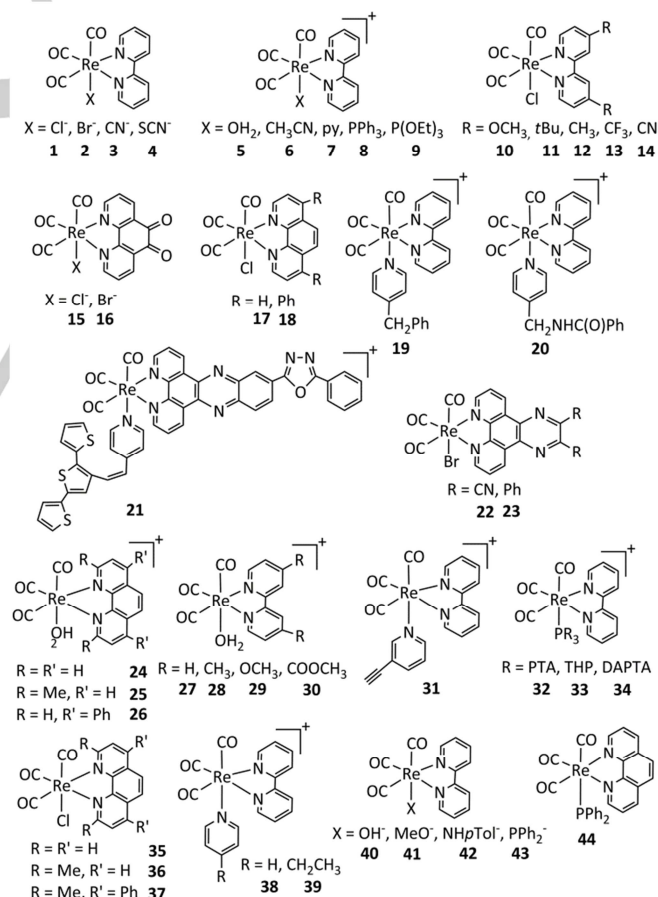**Abstract:** Reactions between [Re(X)(CO)$_3$(bipy)] (X = OH, OMe, NHpTol, PPh$_2$; bipy = 2,2'-bipyridine) complexes and methyl propiolate (HMAD) are studied to rationalize the different products experimentally obtained. Three reaction patterns were found with a common and limiting initial attack of X to HMAD. Thus, the experimental selectivity depends on the kinetics and/or thermodynamics of the last reaction stages. For X = OH and NHpTol an easy intramolecular attack of the X-linked HMAD to a highly electrophilic CO ligand is followed by a hydrogen transposition to this CO, yielding very stable species (C-C_{COH} products). When X = OMe, the insertion of the X-attached HMAD into the Re-OMe bond (*ins* product) takes place due to the smallest barrier and the largest stability of the *ins* route. Finally, when X = PPh$_2$ the *ins* route becomes restricted and the route for the coupling of the X-attached HMAD with bipy (C-C_{bipy} product) wins over the one for the coupling with CO (C-C_{CO} product) only due to the larger stability of the C-C_{bipy} product.

Introduction

Rhenium(I) tricarbonyl complexes of the general formula *fac*-[Re(CO)$_3$(N-N)L]^n, where N-N is a 2,2'-bipyridine or 1,10-phenanthroline-based diimine ligand and L is neutral (n = +1) or anionic (n = 0) monodentate ligand, are involved in numerous, diverse, and important applications. Among others, that kind of Re compounds has been investigated as photocatalysts and/or electrocatalysts for reducing CO$_2$ and H$^+$ (**1-16** in Scheme 1),[1-18] molecular sensors or photoswitches (**16-20** in Scheme 1),[19-26] emitting centers in organic light-emitting diodes (**1**, **11**, **12**, **17**, **18**, and **21-23** in Scheme 1),[27] anticancer agents (**15** and **24-34** in Scheme 1),[28-34] cellular and biomolecular imaging agents (**1**, **2**, and **35-39** in Scheme 1),[35-46] or reagents for synthesizing new organometallic compounds (**3**, **4**, and **40-44** in Scheme 1).[47-54] These applications can be adjusted by choosing the diimine ligand N-N or the monodentate ligand L with the appropriate substituents. Besides this, the changes in the non-carbonyl ligands of the Re(I) complexes can also drastically

modify their reactivity towards other molecular systems. Particularly, several experimental findings have shown that the reaction between the complexes [Re(X)(CO)$_3$(N-N)] (X = OH (hydroxo), OMe (methoxo), NHpTol (*para*-tolylamido), PPh$_2$ (diphenylphosphanido); N-N = 2,2'-bipyridine (bipy); 1,10-phenanthroline (phen)) and activated alkynes like methyl propiolate (HMAD) or dimethylacetylenedicarboxylate (DMAD) gives rise to the formation of different reaction products.[47,49-52] The product formed depends on the nucleophilic ligand (X) used, rather than the bidentate ligand of the metal complex (see below). Molybdenum(II) complexes of type [Mo(η^3-allyl)(X)(CO)$_2$(N-N)] (X = OH, OMe, NHpTol; N-N = bipy, phen) have also shown the same reactivity patterns against activated alkynes as their Re(I) analogues.[47-52]

[a]   D. Álvarez, Dr. M. I. Menéndez, Dr. R. López
       Departamento de Química Física y Analítica
       Universidad de Oviedo
       C/ Julián Clavería 8, 33006 Oviedo, Asturias, Spain
       E-mail: rlopez@uniovi.es

[b]   Dr. J. Díaz
       Departamento de Química Orgánica e Inorgánica
       Universidad de Extremadura
       Avenida de la Universidad s/n, 110071 Cáceres, Extremadura, Spain

       Supporting information for this article is given via a link at the end of the document.

Scheme 1. Basic structures of rhenium(I) tricarbonyldiimine complexes containing neutral or anionic monodentante ligands involved in diverse applications.

FULL PAPER

According to experimental findings, it has been suggested that all reactions between [Re(X)(CO)₃(N–N)] and activated alkynes start with an initial attack of the nucleophilic ligand X to one of the acetylenic carbon atoms to form a zwitterionic intermediate (I in Scheme 2).[51,52] In this scheme, X was replaced by YR to better follow the formation of the different types of reaction products. In the amido and hydroxo complexes the just added alkyne binds to a CO ligand in *cis* disposition (*see* P*cco* species in Scheme 2) and transposition of a proton from the nucleophilic ligand to the attacked CO takes place (*C-C_CO* route and P*ccoh* product in Scheme 2).[49,50] Alternatively, in the alkoxo complex the alkyne inserts into the Re–OMe bond (*ins* route and P*ins* product in Scheme 2).[47] Finally, the phosphanido complex leads to the formation of a different kind of product coming from the addition of the alkyne to the bidentate ligand (*C-C_bipy* route and P*ccb* product in Scheme 2).[51,52] This last reaction is remarkable because of the inertness of coordinated bipy and phen. Furthermore, this result stands in contrast with the P*cco*-type products reported for the reaction towards activated alkynes of Fe, Mo, W, and Ir complexes containing the same PPh₂ phosphanido ligand[55-57] and with P*ins*-type product detected in case of a Nb complex.[58] It is also believed that the reaction of a stannylphosphole complex with DMAD evolves through an intermediate resulting from the alkyne insertion into the P–Sn bond.[59]
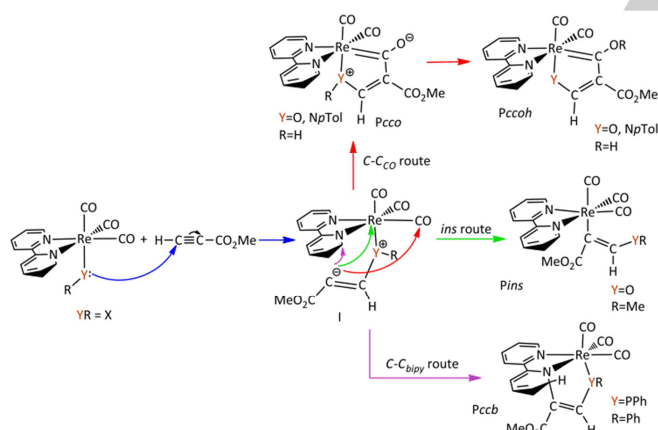
Scheme 2. Reaction mechanisms suggested for the reaction of rhenium(I) tricarbonyl complexes containing a nucleophilic ligand (X) with methyl propiolate (HMAD). For clarity, the YR label for X was used here.

Within this framework, we wondered about the aspects of the nucleophile ligand that are key to obtaining a given product in the reaction of Re(I) complexes and activated alkynes. This is particularly important to get a better understanding of such chemistry, but above all to gather information that could guide a strategy to tune those complexes in order to get new or improved technological, biomedical or chemical synthesis applications. For instance, a systematic modification of the axial ligands to a substituted bipy ligand has allowed for red-shifted absorbance features in Re(I) carbonyl complexes.[60] Computations have been crucial to show that the

aforementioned result is a consequence of destabilization of the Re *d*-orbitals. Therefore, we undertook a comparative theoretical study on the reactivity of [Re(X)(CO)₃(bipy)] (X = OH, OMe, NH*p*Tol, PPh₂) complexes and HMAD. The choice of the simplest bidentate ligand bipy and activated alkyne HMAD in this investigation does not imply a loss of generality of the results obtained, although there is indeed a significant improvement in the computational cost-efficiency ratio. The reactive process involving the PPh₂ ligand had been previously investigated from a theoretical point of view.[61] The reaction mechanism found is closely related to that shown in Scheme 2 (see below) and confirms the product experimentally found. However, the results of this single study are not enough to rationalize the formation of different products when PPh₂ is replaced by OH, OMe or NH*p*Tol. The type of atom directly linked to Re (O, N or P) and/or its substituents (H, Me, H*p*Tol or Ph₂) seem to be responsible for the selectivity of the reaction and, consequently, the present research is needed to clarify their particular effects.

Computational Chemistry Details

Full geometry optimizations of the species involved in the reactive processes between [Re(X)(CO)₃(bipy)] (X = OH, OMe, NH*p*Tol) and HMAD were carried out in tetrahydrofuran (THF, ε = 7.58) solution at the PCM-B3LYP/6-31G+(d,p) (LANL2DZ for Re) level. The nature of the critical structures located on the different potential energy surfaces (PES) investigated was verified by means of harmonic vibrational frequency computations. Normal-mode analysis of the imaginary frequency in the transition states (TS) and intrinsic reaction coordinate (IRC) calculations with the second order Gonzalez-Schlegel integration method[62] were carried out in order to connect each TS to the two associated minima of the proposed mechanism. To get more accurate energies (particularly energy barriers), single-point energy calculations on the PCM-B3LYP/6-31G+(d,p) (LANL2DZ for Re) geometries were performed using the domain localized pair natural orbital-coupled cluster approach with single, double, and perturbative triple excitations (DLPNO-CCSD(T)).[63] The balanced Karlsruhe triple-zeta basis set def2-TZVPP[64] and the conductor-like polarizable continuum model (CPCM)[65] were used in the DLPNO-CCSD(T) computations. All organometallic systems investigated showed T1 diagnostic values less than 0.02,[66] suggesting that a multi-reference treatment is not necessary. In general, DLPNO-CCSD(T) energies are more accurate than B3LYP ones using at least a triple-zeta quality basis set.[67] For comparison purposes, the single-point energy of the species containing the PPh₂ ligand, previously investigated at the PCM-B3LYP/6-311+G(2d,p) (LANL2TZ+*f* for Re)//PCM-B3LYP/6-31+G(d,p) (LANL2DZ for Re) level,[61] was also recomputed at the CPCM-DLPNO-CCSD(T)/def2-TZVPP//PCM-B3LYP/6-31+G(d,p) (LANL2DZ for Re) one (Tables S1-S4 in the Supporting Information). For brevity, henceforth in this work, the levels of theory PCM-B3LYP/6-31+G(d,p) (LANL2DZ for Re) and CPCM-DLPNO-CCSD(T)/def2-TZVPP//PCM-B3LYP/6-31+G(d,p) (LANL2DZ for

FULL PAPER

WILEY-VCH

Re) will be denoted as B3LYP and DLPNO-CCSD(T), respectively.

Thermal free energy corrections in THF solution (G_{therm}) were calculated at the B3LYP level starting with molecular partition functions developed for computing gas-phase thermodynamics properties within the ideal gas, rigid rotor, and harmonic oscillator approximations at a pressure of 1 atm and a temperature of 298.15 K.[68] This is a standard procedure that has proven to be a correct and useful approach.[69] For each species, Gibbs free energy in solution was determined by adding G_{therm} to the highly accurate DLPNO-CCSD(T) energy. Unless stated otherwise, for each reactive process investigated, energies discussed in the following sections are all Gibbs free energies in THF solution referred to the corresponding separate reactants.

In order to shed light on the factors governing the formation of the different products experimentally detected depending on the nucleophilic ligand of the Re complex, we carried out different theoretical analyses on the B3LYP electron density of some of the relevant species. The natural bond orbital (NBO)[70] method was used to obtain net atomic charges (NAC) as implemented in the Gaussian 09 suite of programs.[71] Electron delocalization indexes between two atoms A and B in a molecule, $\delta(A,B) = DI$,[72] were computed using AIMAll program[73] within the framework of Bader's Atoms in Molecules (AIM) theory.[74] The DI is a measure of the number of electrons shared between two atoms and therefore, of the covalency of the bond between them.

All B3LYP computations were carried out with the Gaussian 09 suite of programs,[71] while DLPNO-CCSD(T) calculations employed the ORCA program version 4.0.1[75] and the frozen-core approximation. More technical details on the computational chemistry tools mentioned above as well as a justification for the choice of the DLPNO-CCSD(T) method are included in the Supporting Information.

Results and Discussion

Figure 1 displays the DLPNO-CCSD(T) Gibbs energy profiles obtained for the reaction of [Re(X)(CO)$_3$(bipy)] complexes (X = OH, OMe, NHpTol, PPh$_2$) towards HMAD (more details in Tables S1-S16 in the Supporting Information). The labeling of the theoretically located species is in line with the acronyms used in Scheme 2. So, **I1** identifies the zwitterionic intermediate formed in the initial attack of the nucleophile ligand on the HMAD acetylenic carbon bearing the H atom (C1). **I1'** corresponds to an isomer of **I1** wherein the electron lone pair of the acetylenic carbon bearing the CO$_2$Me group (C2) is oriented towards the plane defined by Re and the bipy ligand. **Pcco**, **Pins**, and **Pccb** are possible products generated through the addition of C2 to a CO ligand, the Re atom, and the bipy ligand, respectively. **Pccoh** is another possible product, only present for X = OH and NHpTol, which is similar to **Pcco** wherein a H atom of the nucleophile ligand has migrated to the attacked carbonyl ligand. As seen in Figure 1, three different reaction patterns are

found. First, for the OH and PPh$_2$ ligands initial reactive approaches between reactants converge to **I1'** after passing through **I1** via the corresponding TSs **TS1** and **TS1_1'**. From **I1'** the reaction path splits into three routes giving rise to **Pcco**, **Pins**, and **Pccb** via the TS **TS2cco**, **TS2ins**, and **TS2ccb**, respectively. For X = OH, **Pcco** undergoes a posterior rearrangement to finally give **Pccoh**. Second, for X = OMe the initial nucleophilic attack also leads to **I1** via **TS1** and then transforms into **Pcco** passing through **TS1_1'**. **Pcco** is the splitting structure towards **Pins** and **Pccb** now. Third, NHpTol ligand yields a different surface where two approaching orientations of the reactants render separate routes starting both with the attack of the nucleophile ligand on C1 at HMAD to give the corresponding zwitterions **I1** and **I1b**. At **I1** the C1-bonded H atom is oriented to the same side of the complex as the pTol substituent whereas the opposite orientation is found at **I1b** (see below). On the one hand, **I1** directly becomes **Pcco**, which in turn can evolve to either **Pins** or **Pccoh**. On the other hand, **I1b** gives rise to **Pccb** after a certain rearrangement.

Let us focus in a comparative way on the formation and rearrangement steps of **I1** (blue line in Figure 1), first, and then on the subsequent routes leading to the addition of the alkyne moiety to CO (red line in Figure 1), the Re ion in an insertion process (green line in Figure 1), and the bidentate ligand bipy (purple line in Figure 1).

a) Formation and rearrangement of the initial intermediate

According to Figure 1, for the reaction of the complexes with X = OH and OMe, the TS for the attack of the X ligand to C1, **TS1**, leading to **I1** competes with the TS for the rearrangement of this intermediate, **TS1_1'**, for being the rate limiting step. In the case of the complexes containing X = NHpTol and PPh$_2$, **TS1** is clearly less stable than **TS1_1'** and ends up being the rate limiting TS. As mentioned above, the complex with NHpTol, presents an alternative reactive approach of the reactants, which is controlled by **TS1b**, a TS analogous to **TS1**. Both TSs present similar relative energies, but the **TS1**-controlled route leads to the very stable product **Pccoh**, the one detected experimentally, while the **TS1b**-controlled route gives rise to **Pccb**, which is 14.5 kcal/mol less stable than **Pccoh**. Therefore, in this scenario, we focus on conducting a detailed comparative analysis of the **TS1** species found for the four complexes (see optimized geometries at Figure 2). The route leading to **Pccb** when X = NHpTol will be described afterwards.

The energy barrier determined by **TS1** increases from PPh$_2$ (17.5 kcal/mol) to NHpTol (22.4 kcal/mol), OMe (25.9 kcal/mol), and OH (27.0 kcal/mol), in good agreement with the well-known observation that large atoms are more easily polarizable, and by extension more nucleophilic than small ones. However, the size of the attacking atom is not the only feature affecting the barrier of the nucleophilic attack. The energy of the HOMO of a nucleophile is directly related to its nucleophilicity, being better nucleophiles those with the largest energy HOMOs (considering the sign). For the initial [Re(X)(CO)$_3$(bipy)] complexes (X = OH,
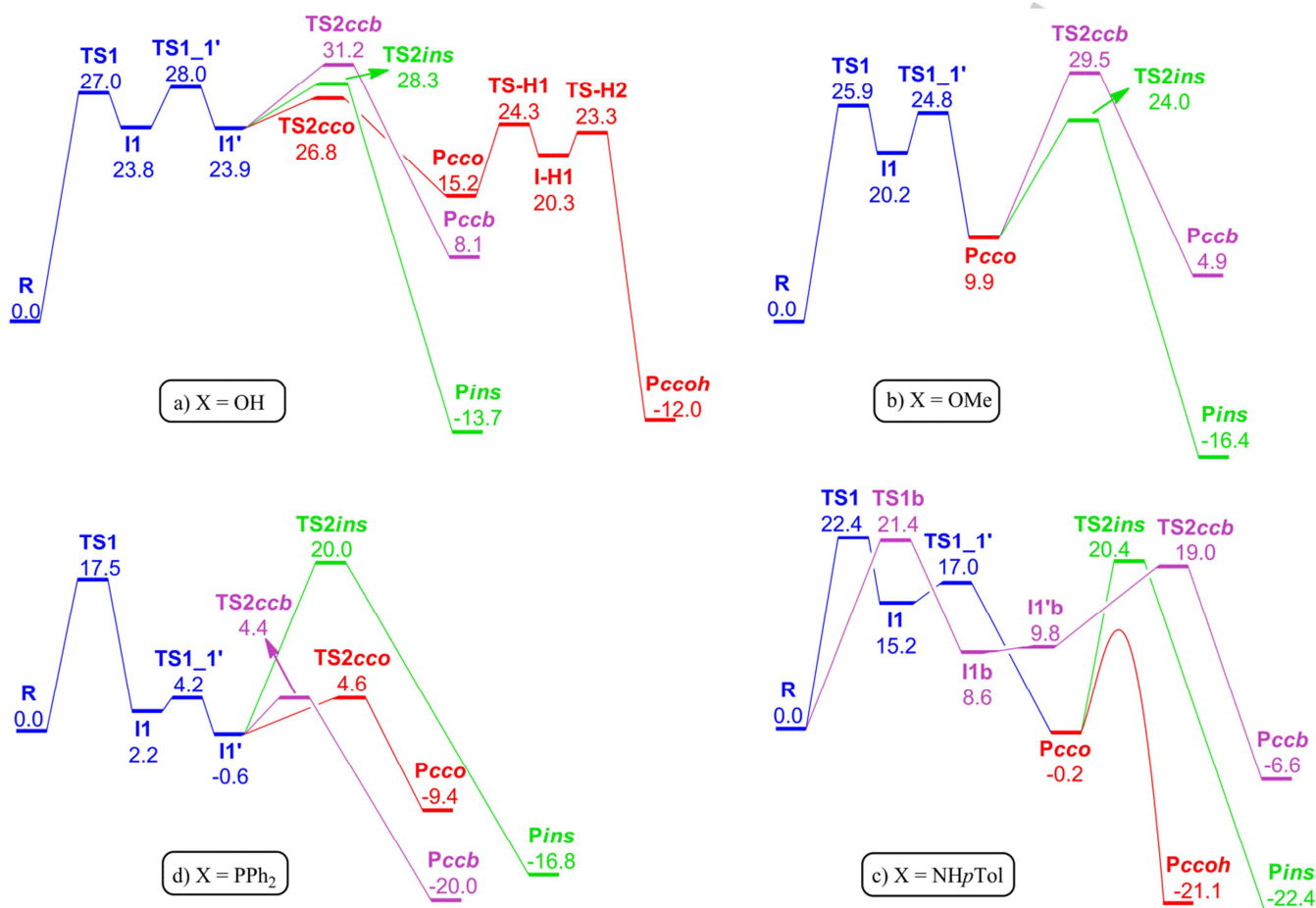
FULL PAPER

WILEY-VCH

Figure 1. DLPNO-CCSD(T) Gibbs energy profiles in kcal/mol for the reaction of [Re(X)(CO)$_3$(bipy)] with HMAD, being X = a) OH, b) OMe, c) NHpTol, and d) PPh$_2$. For **Pcco** and **P$ccoh$** species with X = NHpTol, an approximate connectivity is shown (see text).

OMe, NHpTol, PPh$_2$), **C** in Figure 2, HOMO energies are -0.162 (NHpTol), -0.186 (PPh$_2$), -0.199 (OMe), and -0.208 (OH), all in eV. As seen in Figure 3, the greater stability of the HOMO of the complexes containing OH and OMe can be ascribed to the presence of a notable stabilizing interaction found between a d-type orbital of Re and one of the π^* antibonding orbitals of the CO ligand *trans* to nucleophile ligand. This kind of interaction is notably reduced for complexes containing NHpTol and PPh$_2$. More interestingly, the HOMO energy sequence aforementioned matches the trend in the barriers computationally obtained except when comparing NHpTol and PPh$_2$ with each other. HOMO energies can be understood as a measurement of the general nucleophilicity of the whole complex, where X is one of the ligands. However, electron donation takes place from a particular atom, so the availability of the electron density at this atom is a matter of concern. For the Re complex with X = NHpTol the sum of the three angles centered on N is 359.5°, representative of a planar distribution of groups around N, in good agreement with the value of 359.8° obtained from X-ray

data.[49] The same sum of angles for the complex with X = PPh$_2$ amounts to 319.3°, far from a planar coordination around P (see Figure 2). Both N and P ligands have at least one aromatic group bonded to them. Thanks to the planar coordination and the similar atomic size, the lone pair of the N atom is conjugated with the pTol group, so it is less available for a nucleophilic attack than in the case of the P ligand, where no conjugation between the electron density of the large P atom and any of the Ph groups is present. Actually, the resonance electronic structures where the aromaticity of the pTol ligand is lost contribute to the energy destabilization of the HOMO of the NHpTol ligand. The shape of the HOMO of these two complexes shows the availability of the lone pair of the nucleophile ligand in agreement with previous discussion. As seen in Figure 3, for the complex with PPh$_2$, HOMO is mainly described by the p orbital of the P atom while the one containing NHpTol, the p orbital of the N atom is combined with one of the π bonding orbitals of the pTol substituent.
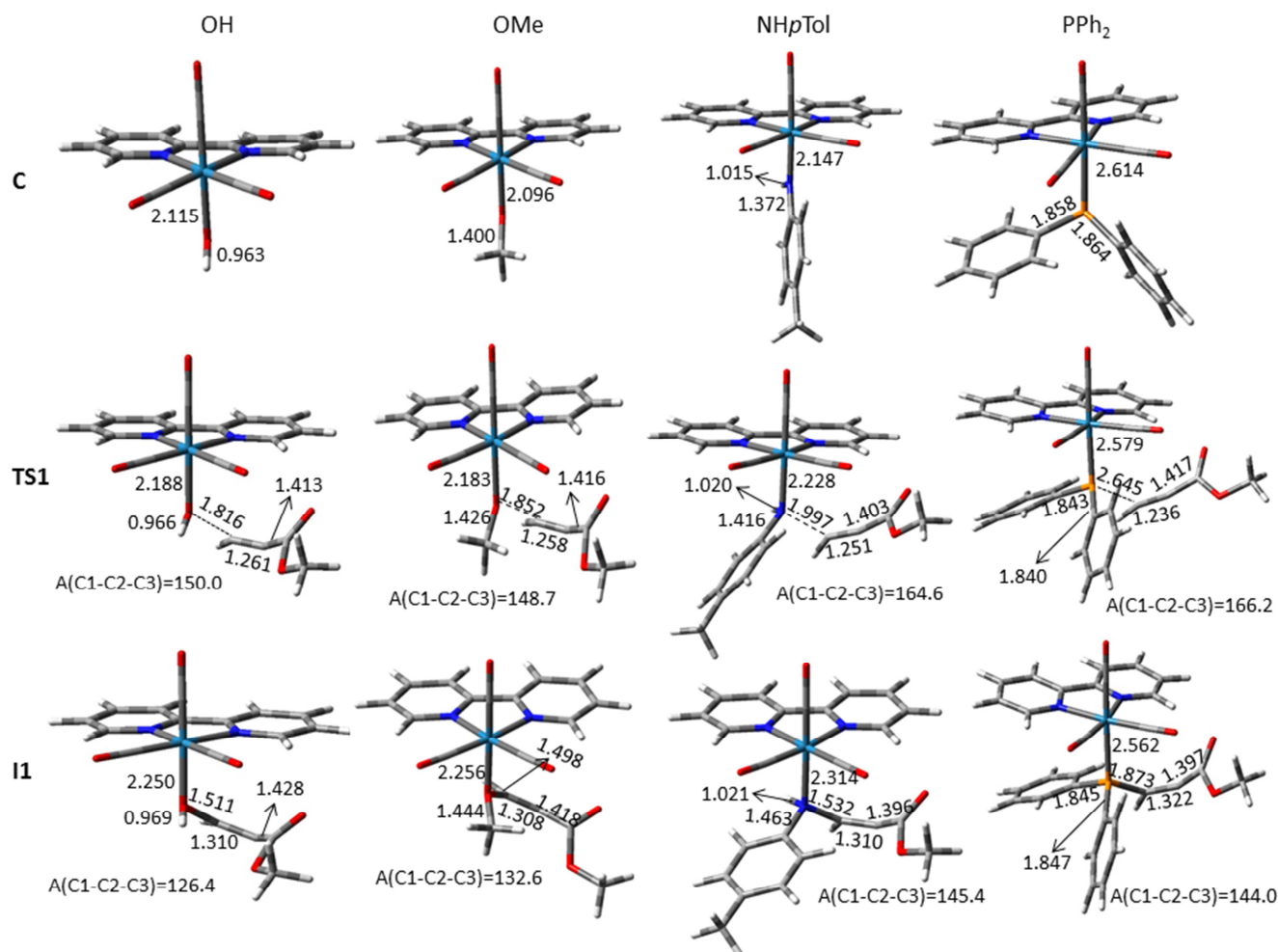
Figure 2. B3LYP optimized structures of the initial [Re(X)(CO)₃(bipy)] complexes (X = OH, OMe, NH*p*Tol, PPh₂), **C**, and the species involved in their nucleophilic attack to HMAD. Relevant bond distances in angstroms and bond angles involving the carbon skeleton of the HMAD moiety, A(HC(1)≡C(2)-C(3)OOCH₃) = A(C1-C2-C3), in degrees are given.

The stability of **I1** with respect to **TS1** amounts to 3.2, 5.7, 7.2, and 15.3 kcal/mol for [Re(X)(CO)₃(bipy)] complexes with X = OH, OMe, NH*p*Tol, and PPh₂, respectively. In this intermediate some electron density has been transferred from the nucleophilic atom of the X ligand to the alkyne (0.275 *e* from O in the OH complex, 0.184 *e* from O in the OMe complex, 0.137 *e* from N, and 0.654 *e* from P, according to NBO population (see Figure S1 in the Supporting Information)) in such a way that a concentration of electron density at C2 has taken place (NAC(C2) = -0.404 *e* for OH complex, -0.388 *e* for OMe complex, -0.317 *e* for NH*p*Tol complex, and -0.245 *e* for PPh₂ complex). At **I1** the incipient lone pair at C2 is in *trans* disposition with respect to the attacking nucleophilic atom and needs to be reoriented towards the equatorial plane of the Re complex where electrophilic positions are placed (see Figure 2). This is done through **TS1_1'**, a broad allene-like TS in the corresponding PES that is 4.2, 4.6, 1.8, and 2.0 kcal/mol larger in energy than **I1** (see Figures 1 and 4) for X

= OH, OMe, NH*p*Tol, and PPh₂, respectively. As already said, complexes with OH and PPh₂ ligands present **I1'** corresponding to a kind of zwitterion stereoisomer of **I1** with the lone pair at C2 in *cis* position with respect to the attacking nucleophilic atom (see Figure 4). NBO charges indicate that both N and P lose electron density when evolving from the initial complexes to **I1** and then to **I1'**, when present. At **I1** with PPh₂ the charge mainly concentrates at C1 of HMAD (NAC(C1) = -0.637 *e*, NAC(C2) = -0.245 *e*), whereas with OH (NAC(C1) = -0.059 *e*, NAC(C2) = -0.404 *e*), OMe (NAC(C1) = -0.047 *e*, NAC(C2) = -0.388 *e*), and NH*p*Tol (NAC(C1) = -0.154 *e*, NAC(C2) = -0.317 *e*,) the electron density is pushed towards C2. However, we note that for the latter the charge concentration at C1 is notably greater than that for the O ligands. For the OMe and NH*p*Tol ligands an exhaustive search through IRC calculations from **TS1_1'** failed to find a similar **I1'** intermediate but led the system to **Pcco**. This particular region of PES seems to be very sensitive to X.
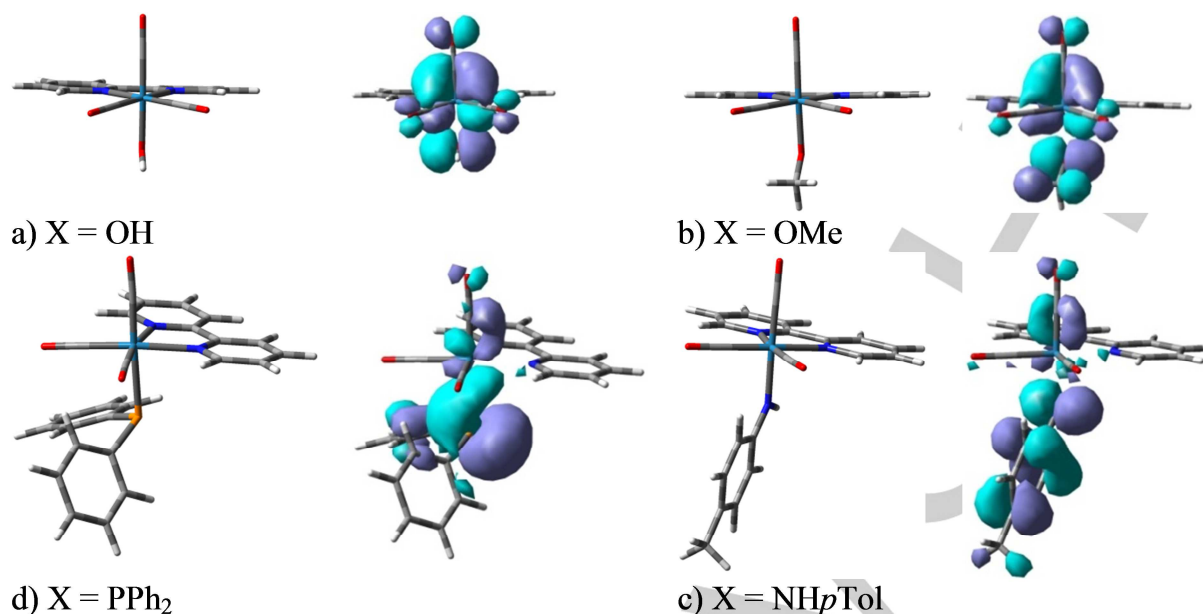
a) X = OH

b) X = OMe

d) X = PPh₂

c) X = NHpTol

Figure 3. Shape of the HOMOs for [Re(X)(CO)₃(bipy)] complexes with X = a) OH, b) OMe, c) NHpTol, and d) PPh₂.
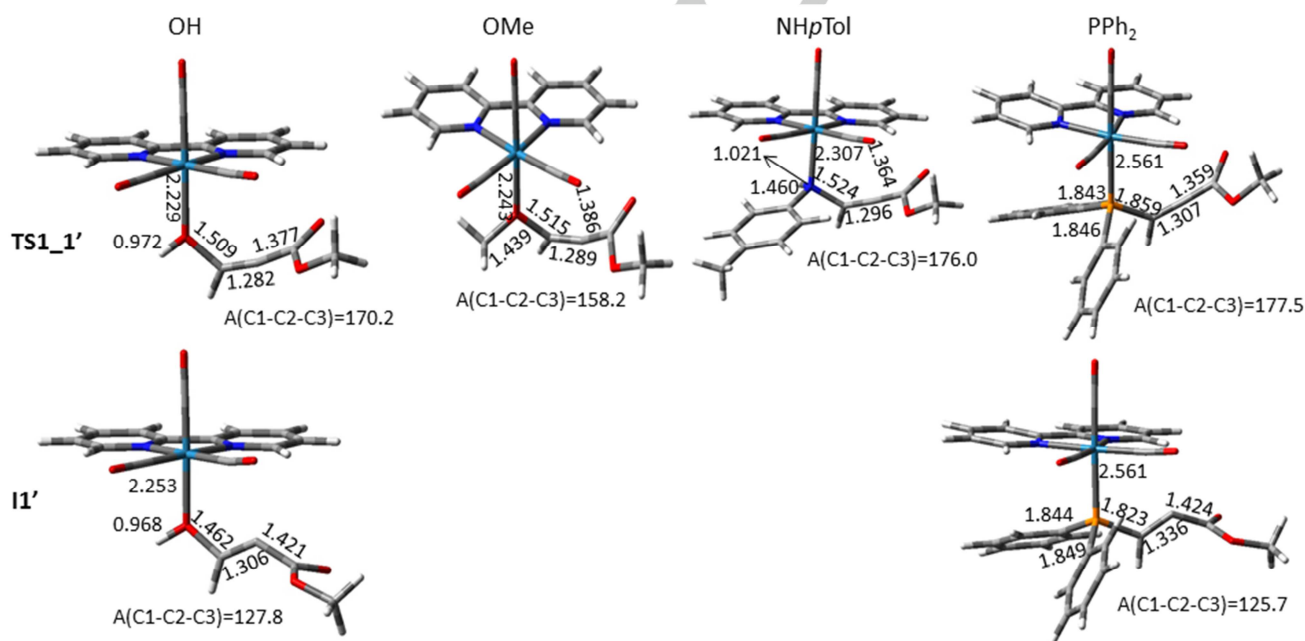

Figure 4. B3LYP optimized structures of **TS1_1'** and **I1'** (when present) for the reaction of [Re(X)(CO)₃(bipy)] (X = OH, OMe, NHpTol, and PPh₂) towards HMAD. Relevant bond distances in angstroms and bond angles involving the carbon skeleton of the HMAD moiety, A(HC(1)≡C(2)-C(3)OOCH₃) = A(C1-C2-C3), in degrees are given.

b) Addition of the alkyne moiety to a CO ligand

As displayed in Figure 1, **I1'** becomes **Pcco** through the TS **TS2cco** for the OH and PPh₂ ligands. However, **Pcco** is obtained from **I1** via **TS1_1'** for OMe and NHpTol. Moreover, for these ligands, **I1'** and **TS2cco** could not be detected after an extensive search.

TS2cco is for the C-C coupling between C2 and a CO ligand in *cis* with respect to the attacking nucleophilic ligand, which leads to the formation of a five-membered ring in a new bidentate ligand. It presents a low barrier of 2.9 kcal/mol (OH) and 5.2 kcal/mol (PPh₂), when measured from **I1'**. According to NBO charges, the CO ligand in *cis* disposition with respect to the alkyne moiety is a strong electrophile due to the large positive
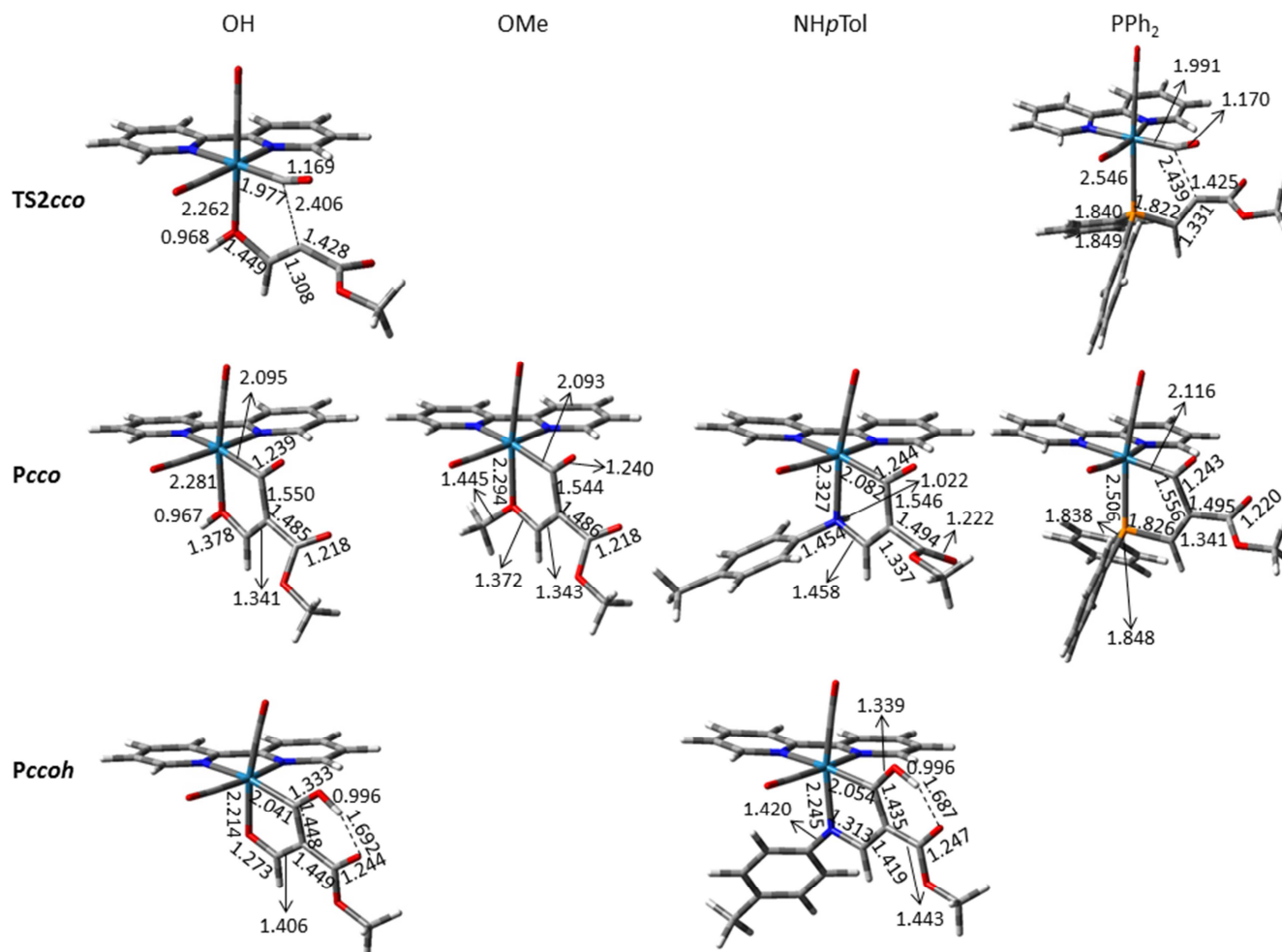
Figure 5. B3LYP optimized structures of **TS2cco**, **Pcco**, and **Pccoh** (when present) for the reaction of [Re(X)(CO)₃(bipy)] (X = OH, OMe, NH*p*Tol, and PPh₂) towards HMAD. Relevant bond lengths in angstroms are displayed.

charge on its C atom (0.730 and 0.756 *e* for OH and PPh₂ ligands at **I1'**, respectively). As seen in Figure 5, both of them are early TSs where the new C2-CO bond is still long (2.406 and 2.439 Å for OH and PPh₂, respectively) and the triple C1-C2 bond still short (1.308 and 1.331 Å for OH and PPh₂, respectively). Geometrically, CO is close to the attacking C2 atom, so both electronic and steric factors point to a small barrier, as it is indeed.

At **Pcco** the alkyne moiety has been fully incorporated to the Re complex through its C1-C2 bond yielding the new five-membered metallacycle (see Figure 5). The Gibbs energy of **Pcco** is larger than that of isolated reactants for OH (15.2 kcal/mol) and OMe (9.9 kcal/mol) complexes, but smaller for NH*p*Tol (-0.2 kcal/mol) and PPh₂ (-9.4 kcal/mol) complexes. It is interesting to note that the Re-X distance at **Pcco** is about 8.5% longer than in isolated reactants for OH, OMe, and NH*p*Tol ligands, whereas it becomes reduced by about 4% at **Pcco** for the PPh₂ complex. The strengthening of the Re-P bond seems

to provide extra stability to this last **Pcco** product. In the case of Re(I) complexes with the OH and NH*p*Tol ligands, both containing a H atom bonded to a nucleophilic atom, **Pcco** evolves to a new product where that H atom has migrated to the O atom of the attacked CO ligand (see **Pccoh** in Figure 5). The transformation **Pcco → Pccoh** could occur via an intramolecular hydrogen shift. Several options were considered, but none of them proved feasible (see discussion and Figure S2 in the Supporting Information), so, we figured it could take place through an intermolecular hydrogen shift. Figure 6 displays the main structures located for the OH ligand and Tables S5-S7 collect their energy data. The process starts with the species **Pcco_dimer** where two **Pcco** moieties oriented themselves with the H atoms of the OH ligands heading to the carbonyl oxygen atoms of the ester groups of the opposite molecule. Then, **TS-H1** performs the simultaneous transfer of both H atoms with a Gibbs energy barrier of 9.1 kcal/mol from **Pcco_dimer** to give rise to intermediate **I0-H1**, where the carboxylate groups hold

the travelling hydrogen atoms at a distance of 1.010 Å. From **I0-H1** several low energy demanding rearrangements place the transferred H atom closer to the attacked carbonyl ligand, as shown in the monomer species **I-H1**. Finally, the last step in the H migration occurs through **TS-H2** where the migrated hydrogen rotates and transfers to the target CO, leading to a new stabilizing H-bond with the ester group. Geometrically, the metallacyle at **P*ccoh*** products is tighter than that at the corresponding **P*cco*** previous species (see Figure 5). Only the C1-C2 bond slightly elongates. These issues, along with the absence of charges of **P*ccoh*** products, make them the second

most stable ones (after **P*ins***) for the reaction of these complexes (-12.0 and -21.1 kcal/mol for OH and NH*p*Tol ligands, respectively). Analogous dimer intermediates and reaction path are assumed to describe the H transfer between **P*cco*** and **P*ccoh*** for the complex with NH*p*Tol. Although the notable size of the dimer systems containing this ligand prevents the performance of the very demanding DLPNO-CCSD(T) calculations, the similarity of the species found for the intramolecular hydrogen migration to those for the OH ligand seems to validate our assumption (see Supporting Information).
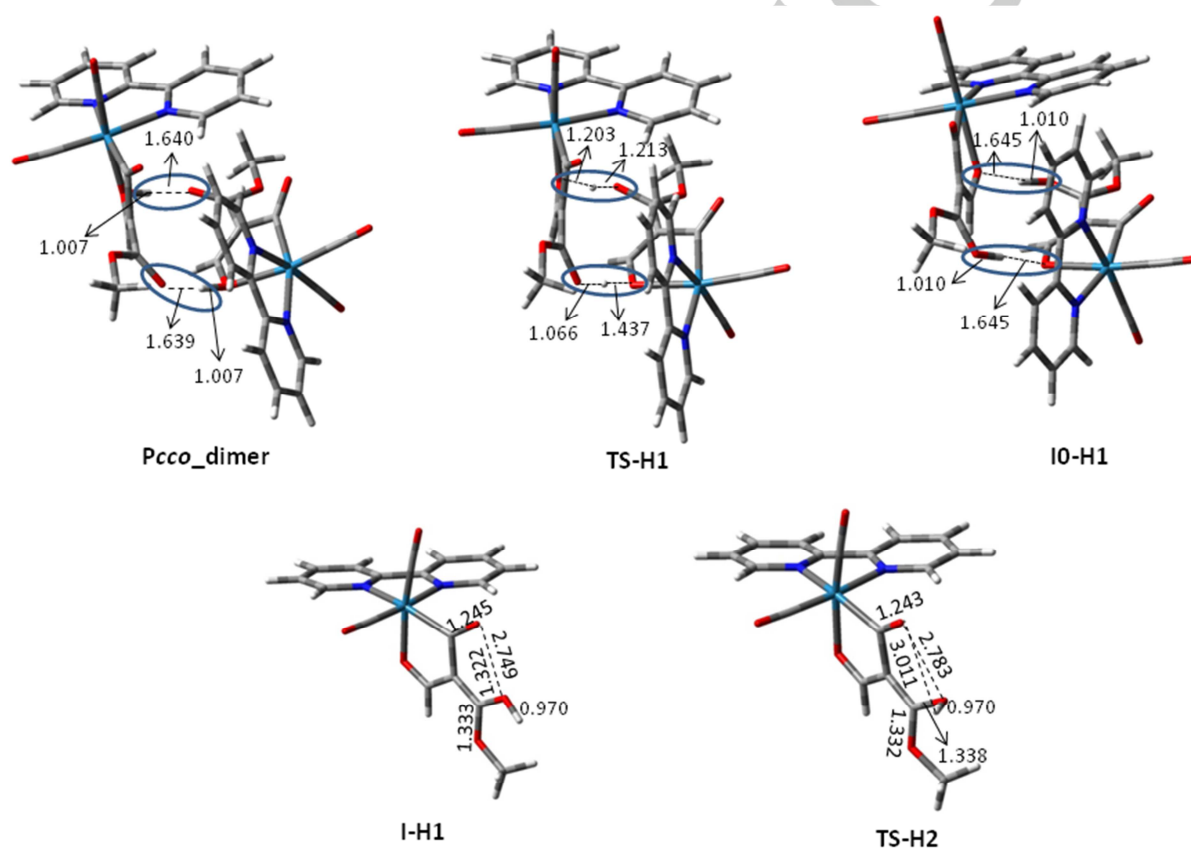

Figure 6. B3LYP optimized structures for the H transpositions from the OH ligands to the carbonyl oxygen atoms in the **P*cco*** structures. Relevant bond lengths in angstroms are displayed.

c) Addition of the alkyne moiety to the Re atom: the *ins* route

The C2 atom of either **I1'** or **P*cco*** species could also bond to the Re metal evolving through **TS2*ins*** (see Figure 7). At the intermediates previous to **TS2*ins*** the corresponding Re-X bond is strong and starts weakening when the new C2-Re bond begins to form during the concerted synchronous process characterized by **TS2*ins***. For the complex with X = OH, the barrier for **TS2*ins*** is just 4.4 kcal/mol, from **I1'**. Such a small

value indicates that the energy released from the partial formation of the new C2-Re bond nearly compensates for the cost of breaking the Re-O bond. A different situation appears for the complex with X = PPh$_2$, where the barrier for **TS2*ins*** raises to 20.6 kcal/mol from its previous intermediate, **I1'**. This means that the Re-P bond is much stronger than the bond formed between Re and O in the X = OH complex considered here. Actually, the DI shows a value of 0.614 for the Re-P bond, notably larger than that found for the Re-O one (0.374). The *d* orbitals in a third-row atom, like phosphorous, are better sized to largely overlap with Re ones than second-row atoms. This

makes the insertion path very unlikely for the complex with the PPh$_2$ ligand. On the other hand, in complexes with X = OMe and NHpTol IRC calculations clearly demonstrate that **Pcco** is the structure preceding **TS2ins**, with a barrier of 14.1 and 20.6 kcal/mol respectively, measured from it. These large values come from the fact that two bond breakages are needed to accomplish the insertion, the Re-O or Re-N and the C2-CO ones. The products formed at the end of this reaction path are *Z*-alkenyl complexes with no charge separation. This explains why

this type of products is more stable than reactants (between 13 and 17 kcal/mol for OH, OMe, and PPh$_2$ systems and 22.4 kcal/mol for NHpTol). In the case of NHpTol the aromatic ring bonded to the N atom is placed far away from the complex equatorial ligands, thus avoiding repulsive interactions present in the remaining structures of its reaction profile. It has been reported that, when the insertion product is the main one, addition of an acid like HTOf in CDCl$_3$ allows the release of the corresponding *Z*-alkenyl complex with H replacing the metal.[47]
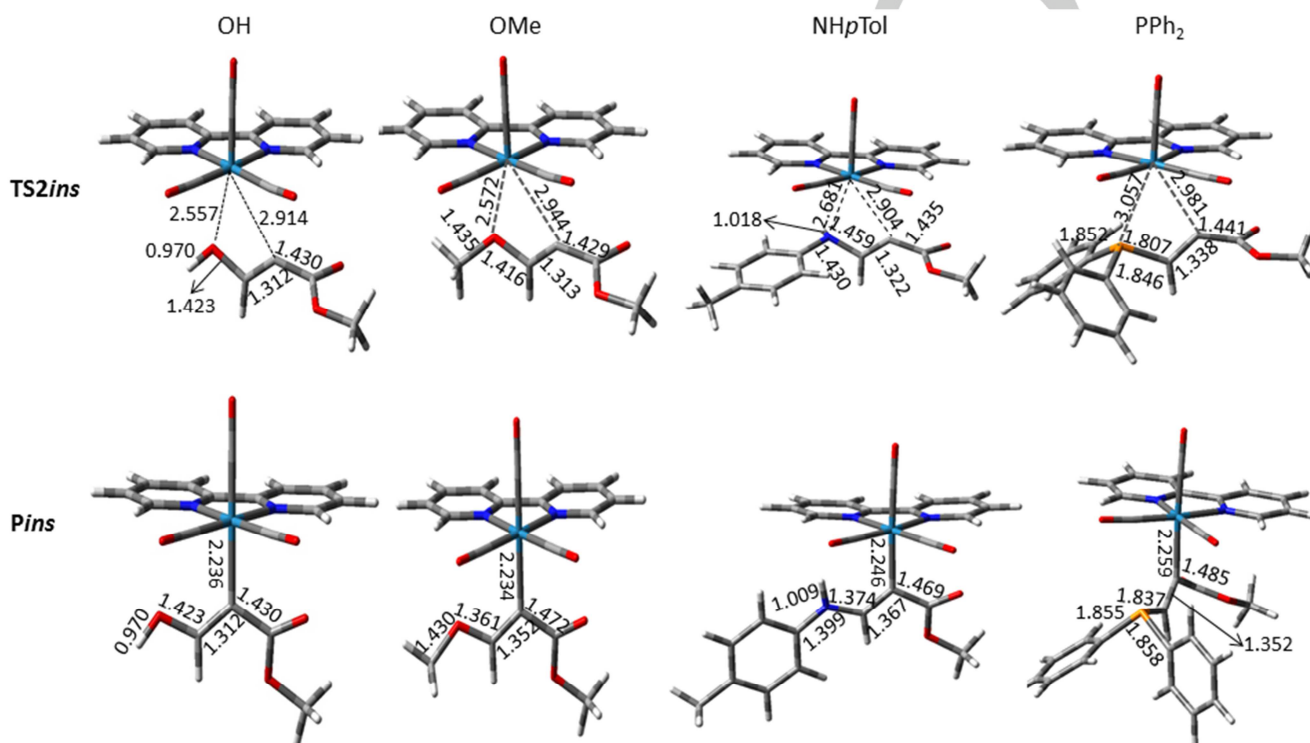

Figure 7. B3LYP optimized structures of the species involved in the addition step to the Re atom for the reaction of [Re(X)(CO)$_3$(bipy)] (X = OH, OMe, NHpTol, and PPh$_2$) towards HMAD. Relevant bond lengths in angstroms are shown.

d) Addition of the alkyne moiety to the bipy ligand

Although hardly electrophilic, one of the *ortho* C atoms bearing a hydrogen at the bipy ligand, C6, could also be attacked by the C2 alkyne atom, as it was experimentally observed for the complex with PPh$_2$ ligand.[51,52] **TS2ccb** represents this addition and has been theoretically characterized for the four complexes here considered (see Figures 8 and 9). However, three different reaction paths are computationally observed for the formation of **Pccb**. As for **TS2ins**, **TS2ccb** may come from **I1'** (complexes with X = OH and PPh$_2$) or **Pcco** (complex with X = OMe). However, for the complex with X = NHpTol IRC calculations indicate that a slightly different zwitterion, **I1'b**, is preceding **TS2ccb**. At **I1'b** the C1-bonded hydrogen atom of the alkyne moiety (H1) is placed *outwards* with respect to the bidentate ligand (see Figure 8), which suggests an approach of the reactants different from that considered so far. Actually, leaving

H1 *outwards* at the initial interaction between reactants leads to a TS, **TS1b**, with nearly the same energy as **TS1** that evolves to **I1b** (see Figure 8). This intermediate resembles **I1** in the sense that the lone pair that starts forming at C2 is in *trans* disposition with respect to the attacking N atom, but **I1b** is 6.6 kcal/mol more stable than **I1**. No TS but a steadily decreasing energy path joins **I1b** with **I1'b**, where the lone pair at C2 is in *cis* orientation with respect to the nucleophilic N atom. **I1'b** resembles intermediates **I1'** found for the rest of complexes in the sense that some electron density concentrates on the C2 atom of the alkyne (-0.422 e) and faces towards the electron poor area of the equatorial ligands. However, C2 electron charge is pointing to bipy in a more tilted way than in the remaining **I1'** intermediates. **I1'b**, with a relative Gibbs energy of 9.8 kcal/mol, evolves to **TS2ccb** and finally to **Pccb**. The
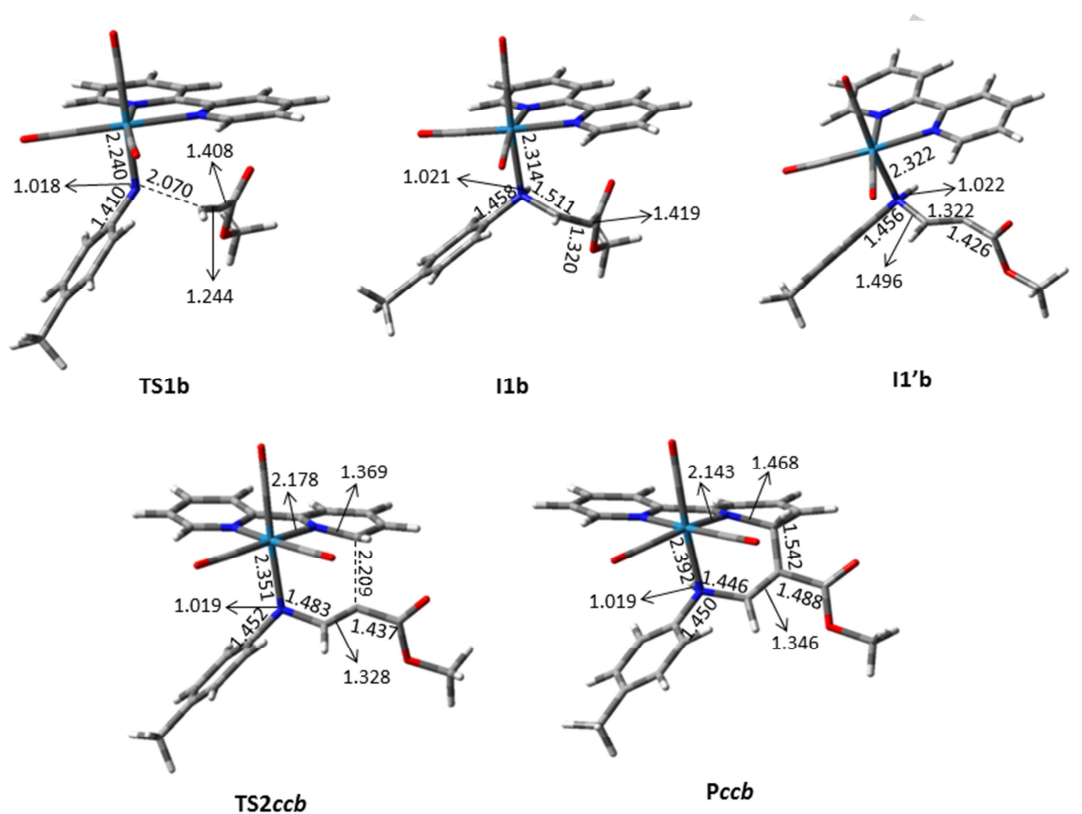
Figure 8. B3LYP optimized structures for the reaction of [Re(NH*p*Tol)(CO)₃(bipy)] with HMAD to yield **P*ccb***. Some relevant distances in angstroms are given.

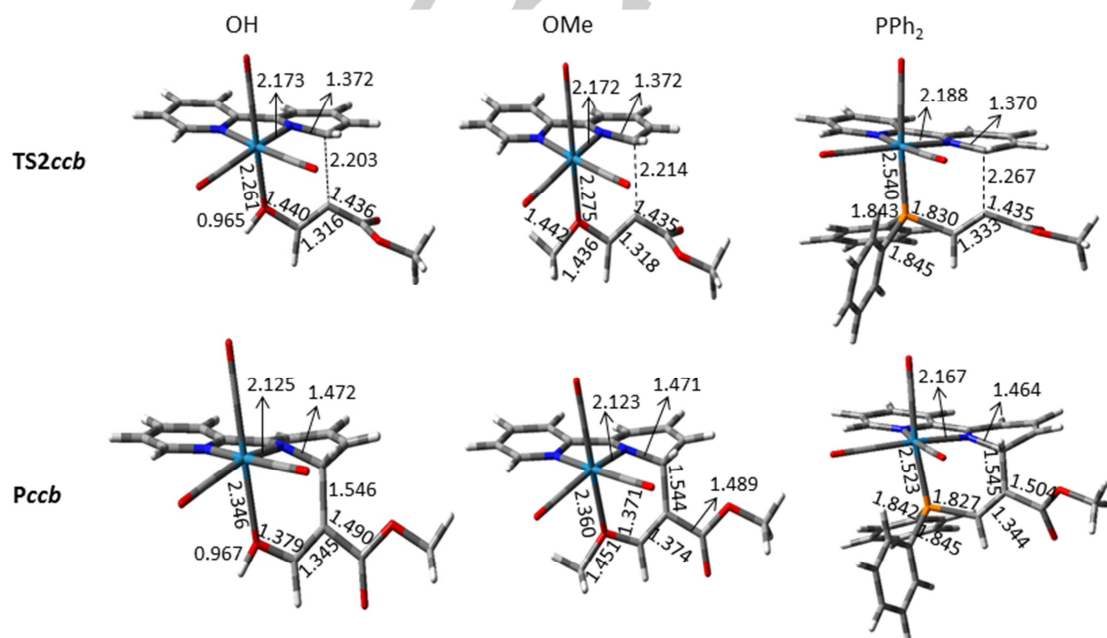**Figure 9.** B3LYP optimized structures of the species implied in the addition step of the alkyne moiety to the bipy ligand for the reaction of [Re(X)(CO)₃(bipy)] (X = OH, OMe, and PPh₂) towards HMAD. Relevant bond distances in angstroms are shown.

FULL PAPER

WILEY-VCH

approach of HMAD to H1 in the *outward* orientation was also found for the rest of the complexes, but did not link to the routes leading to the experimentally observed products.

For complexes with NH*p*Tol and mainly for those with OH and OMe ligands, the barrier of **TS2*ccb*** is large when measured from the reactants (31.2, 29.5, and 19.0 kcal/mol for OH, OMe, and NH*p*Tol systems, respectively) and the **P*ccb*** products present no or low positive Gibbs energy stabilization (8.1, 4.9, and -6.6 kcal/mol for X = OH, OMe, and NH*p*Tol, respectively). Several reasons explain the high instability of **TS2*ccb*** and **P*ccb*** structures for X ligands with a second row element (N or O). First, as seen in Figure S1, the C6 atom of bipy shows a small positive charge at the intermediates preceding **TS2*ccb***, which means that it is a poor electrophile. Second, as it can be seen in Figures 8 and 9, at **TS2*ccb*** a six-membered non-planar metallacycle is starting to form and, as a consequence, the aromaticity in the attacked bipy ring becomes reduced, losing its planarity. When X ligand contains an O atom the C2-C6 bond is shorter, the aromatic ring is more distorted, that is, largest barriers correlate with larger aromaticity reductions. For the **TS2*ccb*** and **P*ccb*** structures when X = OH, OMe, and NH*p*Tol the Re-X bond is considerably longer than in the corresponding reactant complex (see Figure 9). The weakening of the bond with the metal may also contribute to the instability of these structures. When X = PPh$_2$, **TS2*ccb*** presents a barrier of only 4.4 kcal/mol, similar to that of **TS2*cco*** (4.6 kcal/mol) and much smaller than that of the other **TS2*ccb***-type species. The loss of bipy aromaticity seems to be compensated by the formation of a loose six-membered metallacycle where the Re-P bond becomes stronger than in the initial reactant (with a shorter distance), which makes it particularly stable.

e) General discussion of the theoretical results and comparison with the experiment

In spite of the apparent similarity of [Re(X)(CO)$_3$(bipy)] (X = OH, OMe, NH*p*Tol, and PPh$_2$) complexes, it has been experimentally found that the nature of the X ligand determines the formation of different products in their reactivity towards activated alkynes, such as HMAD. The detailed analyses previously done for these reactions confirm experimental observations and shed some light on the reasons under this behavior. Actually, it is shown that the prevalence of one of the three possible products, **P*cco*** (**P*ccoh***, when present), **P*ins*** or **P*ccb***, depends on a subtle balance between the kinetic barriers of the final step of their formation, since the initial nucleophilic approach of the X ligand to the alkyne is common for routes leading to all of the products (see Figure 1), and their associated thermodynamic stability. These facts are not expected to change in the event that HMAD was computationally replaced by symmetric activated acetylenes like DMAD, since this substitution did not modify the kind of reaction product obtained experimentally.[49,51,52] The presence of DMAD will lower the energy barrier of the initial nucleophilic approach to afford **I1** as the acetylenic carbons (C1 and C2) for the isolated DMAD are less electronically populated (~ 0.12 *e*) than the analogous ones for HMAD and also the LUMO of DMAD is lower in energy (0.008 eV) than the analogous one of HMAD (see Table S17). By contrast, a slight increase in energy barriers for the formation of the different reaction products from **I1** is expected, taking into account that C2 in **I1** with DMAD is less electronically populated than that one with HMAD (see **I1** for the NH*p*Tol case in Figure S1 and Table S17). Nonetheless, this will not affect the selectivity of these reactive processes because the NBO charges of the three atoms attacked by C2 (*Re*, *C$_{CO}$*, and *C$_{bipy}$*) are very similar to those found at **I1** with HMAD (compare **I1** in Figure S1 and Table S17).

For X = OH and NH*p*Tol the experimentally observed product is **P*ccoh***.[49,50] The intramolecular addition to an equatorial CO ligand is an easy process for all four Re(I) complexes, to the point that it may not require surpassing a Gibbs energy barrier when X = OMe and NH*p*Tol (**TS2*cco*** was not found for these ligands and instead it is the TS for **I1** rearrangement (**TS1_1'**) that ends up giving rise **P*cco***). However, only **P*cco***-type products are clearly more stable than the separate reactants for the PPh$_2$ ligand and are always less stable than the corresponding **P*ccb*** and **P*ins***-type products. Only when X contains a nucleophilic atom bonded to a H atom (X = OH and NH*p*Tol), the addition to CO is followed by an accessible H transposition that yields the very stable species **P*ccoh*** as the preferred product in accordance with experimental findings.[49,50] For the case of the [Re(NH*p*Tol)(CO)$_3$(bipy)] complex the PES has two different reaction channels from the beginning of the reaction. The channel leading to **P*ccb*** is not competitive with that for the formation of **P*ccoh*** due to the large stabilization of this last product.

For X = OMe the experimentally observed product is **P*ins***.[47] The *ins* route is the most kinetically unfavorable for X = PPh$_2$ due to the strong bond between Re and the third period element, phosphorous, that has to be broken at **TS2*ins***; is kinetically unfavorable for X = OMe and NH*p*Tol due to fact that the structure previous to **TS2*ins***, **P*cco***, needs to break two bonds (Re-O/N and C2-CO) to yield the corresponding **P*ins***; and becomes more favorable for X = OH from **I1'** intermediate, where only the Re-O bond has to be broken. Thermodynamically, the *ins* route is favorable, since it yields very stable products with no charge separation for all complexes. For the particular case of the reaction of [Re(OMe)(CO)$_3$(bipy)] with HMAD, the lower Gibbs energy barrier of **TS2*ins*** compared to its potential competitor **TS2*ccb*** determines, according to experimental evidences,[47] the formation of **P*ins*** as the main reaction product (besides the large thermodynamic stability of the insertion product **P*ins***).

Eventually, for the complex with the PPh$_2$ ligand, intermediate **I1'** exists and is the separation point for the independent routes leading to each of the products (**P*cco***, **P*ins*** or **P*ccb***) via the corresponding TS (**TS2*cco***, **TS2*ins*** or **TS2*ccb***). Compared to X = OH, OMe, NH*p*Tol, the presence of a larger nucleophilic atom at the X ligand like phosphorous relieves the ring strain of the four, five, and six-member metallacycles at **TS2*ins***, **TS2*cco***, and **TS2*ccb***, respectively. This causes an important stabilization of **TS2*cco*** and **TS2*ccb***, and to a much lesser extent **TS2*ins*** due to the strength of the Re-P bond. As a result, the addition routes to CO and bipy, kinetically similar, are much more

favorable than the insertion one. The largest stability of the **P*ccb*** product determines a preference for the formation of **P*ccb***, as experimentally observed.[51,52] Except for the complex with X = PPh$_2$, the route for the coupling with the bipy ligand (C-C_{bipy}) is quite unfavorable both kinetically and thermodynamically.

As just said, the formation of the products experimentally detected, **P*ccoh*** (C-C_{COH} coupling product) for OH and NHpTol, **P*ins*** (insertion product) for OMe, and **P*ccb*** (C-C_{bipy} coupling product) for PPh$_2$, could be rationalized in this work and some reactivity guidelines seem to be emerging. The understanding of the independent or combined effects of the heteroatoms and their substituents at the X ligand on this reactivity will benefit from a systematic study involving complexes not yet experimentally tested that is under way in our laboratory.

Conclusions

A comparative mechanistic study on the reactions of [Re(X)(CO)$_3$(bipy)] (X = OH, OMe, NHpTol, PPh$_2$; bipy = 2,2'-bipyridine) towards methyl propiolate (HMAD) was carried out at the CPCM-DLPNO-CCSD(T)/def2-TZVPP//PCM-B3LYP/6-31+G(d,p)-LANL2DZ level of theory to understand the effect of ligand X on the selectivity of the reaction. Three different reaction patterns were found having in common the initial nucleophilic attack of the X ligand on the terminal acetylenic carbon of HMAD. First, for OH and PPh$_2$ initial reactive approaches lead to the formation of a zwitterionic intermediate that subsequently becomes an isomeric zwitterion. This species is the splitting point for the reaction paths leading to three possible products: the addition of the X-bonded acetylene to one of the CO ligands in *trans* disposition to the bipy one (C-C_{CO} coupling product), the Re atom in an insertion process (*ins* product) or the bipy ligand (C-C_{bipy} coupling product). Second, for OMe, the zwitterion formed at the first step evolves directly to the C-C_{CO} coupling species, which is the splitting structure towards the *ins* and C-C_{bipy} products. Third, for NHpTol two approaching orientations of the reactants render separate routes, one leading to the C-C_{bipy} product and the other to the C-C_{CO} product to which, the *ins* product is linked. In addition, for X ligands containing a hydrogen atom bonded to the nucleophilic atom, OH and NHpTol, we have found an intermolecular mechanism for the evolution of C-C_{CO} species evolves to a more stable one, C-C_{COH} product, where that H atom has shifted to the oxygen atom of the attacked carbonyl ligand. According to our computations, the ester group in HMAD plays a two-fold role by activating the alkyne for the initial nucleophilic addition and by assisting an intermolecular hydrogen migration from C-C_{CO} to C-C_{COH} species in these complexes.

The reaction rate of the reactive processes investigated is determined by the initial nucleophilic attack step. Since this step is common for all the reactions, the preferred product depends on the kinetics and/or thermodynamics ascribed to the last part of the corresponding reaction profile. The formation of C-C_{CO} species is kinetically more favored than that of C-C_{bipy} and *ins* ones, except for X = PPh$_2$ where the energy barriers for the

generation of C-C_{CO} and C-C_{bipy} species compete with each other. By contrast, thermodynamics always favors the formation of *ins*, C-C_{bipy} or, when present, C-C_{COH} species over the C-C_{CO} one. Specifically, when X = OH and NHpTol, an easy intramolecular attack of the HMAD that was just linked to a highly electrophilic CO equatorial ligand is followed by the formation of the very stable C-C_{COH} products. When X = OMe, the *ins* product forms thanks to the smaller barrier and the larger stability of the *ins* route compared to that of its potential competitor, the C-C_{bipy} product. Finally, when X = PPh$_2$ the *ins* route becomes restricted and, therefore the C-C_{bipy} coupling wins over the C-C_{CO} one, but only for the largest stability of the C-C_{bipy} product. Based on this, the products experimentally detected, C-C_{COH} for OH and NHpTol, *ins* for OMe, and C-C_{bipy} for PPh$_2$, could be rationalized and some general reactivity trends have been unveiled. Therefore, the information collected can help design new rhenium carbonyl complexes and other related systems with improved technological, biomedical or chemical synthesis applications.

Acknowledgments

[1] J. Hawecker, J. M. Lehn, R. Ziessel, *J. Chem. Soc., Chem. Commun.* **1983**, 536-538.
[2] J. Hawecker, J. M. Lehn, R. Ziessel, *J. Chem. Soc., Chem. Commun.* **1984**, 328-330.
[3] B. P. Sullivan, C. M. Bolinger, D. Conrad, W. J. Vining, T. J. Meyer, *J. Chem. Soc., Chem. Commun.* **1985**, 1414-1416.
[4] J. Hawecker, J. M. Lehn, R. Ziessel, *Helv. Chim. Acta* **1986**, *69*, 1990-2012.
[5] Y. Hayashi, S. Kita, B. S. Brunschwig, E. Fujita, *J. Am. Chem. Soc.* **2003**, *125*, 11976-11987.
[6] P. Kurz, B. Probst, B. Spingler, R. Alberto, *Eur. J. Inorg. Chem.* **2006**, 2966-2974.
[7] H. Takeda, K. Koike, H. Inoue, O. Ishitani, *J. Am. Chem. Soc.* **2008**, *130*, 2023-2031.
[8] B. Probst, A. Rodenberg, M. Guttentag, P. Hamm, R. Alberto, *Inorg. Chem.* **2010**, *49*, 6453-6460.
[9] J. M. Smieja, C. P. Kubiak, *Inorg. Chem.* **2010**, *49*, 9283-9289.
[10] H. Takeda, O. Ishitani, *Coord. Chem. Rev.* **2010**, *254*, 346-354.
[11] B. Probst, M. Guttentag, A. Rodenberg, P. Hamm, R. Alberto, *Inorg. Chem.* **2011**, *50*, 3404-3412.
[12] K. A. Grice, C. P. Kubiak, A. Michele, E. van Rudi, *Adv. Inorg. Chem.* **2014**, *66*, 163-188.

WILEY-VCH

[13] J. J. Teesdale, A. J. Pistner, G. P. A. Yap, Y. Z. Ma, D. A. Lutterman, J. Rosenthal, *Catal. Today* **2014**, *225*, 149-157.

[14] C. Matlachowski, B. Braun, S. Tschierlei, M. Schwalbe, *Inorg. Chem.* **2015**, *54*, 10351-10360.

[15] T. W. Schneider, M. Z. Ertem, J. T. Muckerman, A. M. Angeles-Boza, *ACS Catal.* **2016**, *6*, 5473-5481.

[16] C. Kefalidi, E. Koutsouri, L. Marchiò, A. Zarkadoulas, S. Efstathiadou, C. A. Mitsopoulou, *Polyhedron* **2016**, *110*, 157-164.

[17] E. Koutsouri, C. A. Mitsopoulou, *Open Chem.* **2016**, *14*, 393-403.

[18] M. L. Clark, P. L. Cheung, M. Lessio, E. A. Carter, C. P. Kubiak, *ACS Catal.* **2018**, *8*, 2021-2019.

[19] D. B. MacQueen, K. S. Schanze, *J. Am. Chem. Soc.* **1991**, *113*, 6108-6110.

[20] K. S. Schanze, D. B. MacQueen, T. A. Perkins, L. A. Cabana, *Coord. Chem. Rev.* **1993**, *122*, 63-89.

[21] S. S. Sun, A. J. Lees, *J. Am. Chem. Soc.* **2000**, *122*, 8956-8967.

[22] M. Bakir, *Acta Crystallogr., Sect. C: Struct. Chem.*, **2001**, *57*, 1371-1373.

[23] A. S. Polo, M. K. Itokazu, K. M. Frin, A. O. de T. Patrocínio, N. Y. M. Iha, *Coord. Chem. Rev.* **2006**, *250*, 1669-1680.

[24] D. Pelleteret, N. C. Fletcher, A. P. Doherty, *Inorg. Chem.* **2007**, *46*, 4386-4388.

[25] M. C. L. Yeung, V. W. W. Yam, *Chem. Soc. Rev.* **2015**, *44*, 4192-4202.

[26] A. Zarkadoulas, E. Koutsouri, C. Kefalidi, C. A. Mitsopoulou, *Coord. Chem. Rev.* **2015**, *304-305*, 55-72.

[27] (a) N. J. Lundin, A. G. Blackman, K. C. Gordon, D. L. Officer, *Angew. Chem. Int. Ed.*, **2006**, *45*, 2582-2584. (b) G. W. Zhaoa, J. H. Zhaoa, Y. X. Hua, D. Y. Zhangb, X. Lia, *Synth. Met.* **2016**, *212*, 131-141.

[28] G. Gasser, I. Ott, N. Metzler-Nolte, *J. Med. Chem.* **2011**, *54*, 3-25.

[29] A. Leonidova, V. Pierroz, L. A. Adams, N. Barlow, S. Ferrari, B. Graham, G. Gasser, *ACS Med. Chem. Lett.* **2014**, *5*, 809-814.

[30] A. Leonidova, G. Gasser, *ACS Chem. Biol.* **2014**, *9*, 2180-2193.

[31] M. Kaplanis, G. Stamatakis, V. D. Papakonstantinou, M. Paravatou-Petsotas, C. A. Demopoulos, C. A. Mitsopoulou, *J. Inorg. Biochem.* **2014**,*135*, 1-9.

[32] R. R. Ye, C. P. Tan, M. H. Chen, L. Hao, L. N. Ji, Z. W. Mao, *Chem. Eur. J.* **2016**, *22*, 7800-7809.

[33] K. M. Knopf, B. L. Murphy, S. N. MacMillan, J. M. Baskin, M. P. Barr, E. Boros, J. J. Wilson, *J. Am. Chem. Soc.* **2017**, *139*, 14302-14314.

[34] S. C. Marker, S. N. MacMillan, W. R. Zipfel, Z. Li, P. C. Ford, J. J. Wilson, *Inorg. Chem.* **2018**, *57*, 1311-1331.

[35] M. Salmain, M. Gunn, A. Gorfti, S. Top, G. Jaouen, *Bioconjugate Chem.* **1993**, *4*, 425-433.

[36] W. B. Connick, A. J. DiBilio, M. G. Hill, J. R. Winkler, H. B. Gray, *Inorg. Chim. Acta* **1995**, *240*, 169-173.

[37] T. A. Oriskovich, P. S. White, H. H. Thorp, *Inorg. Chem.* **1995**, *34*, 1629-1631.

[38] K. K.-W. Lo, W.-K. Hui, C.-K. Chung, K. H.-K. Tsang, T. K.-W. Lee, C.-K. Li, J. S.-Y. Lau, D. C.-M. Ng, *Coord. Chem. Rev.* **2006**, *250*, 1724-1736.

[39] C. Beck, J. Brewer, J. Lee, D. McGraw, B. A. DeGraff, J. N. Demas, *Coord. Chem. Rev.* **2007**, *251*, 546-553.

[40] K. K.-W. Lo, M.-W. Louie, K.-S. Sze, J. S.-Y. Lau, *Inorg. Chem.* **2008**, *47*, 602-611.

[41] V. Fernández-Moreira, F. L. Thorp-Greenwood, M. P. Coogan, *Chem. Commun.* **2010**, *46*, 186-202.

[42] K. K.-W. Lo, M.-W. Louie, K. Y. Zhang, *Coord. Chem. Rev.* **2010**, *254*, 2603-2622.

[43] K. K.-W. Lo, K. Y. Zhang, S. P.-Y. Li, *Eur. J. Inorg. Chem.* **2011**, 3551-3568.

[44] R. Balasingham, M. P. Coogan, F. L. Thorp-Greenwood, *Dalton Trans.* **2011**, *40*, 11663-11674.

[45] K. K.-W. Lo, A. W.-T. Choi, W. H.-T. Law, *Dalton Trans.* **2012**, *41*, 6021-6047.

[46] J. Skiba, T. Bernas, D. Trzybinski, K. Wozniak, G. Ferraro, D. Marasco, A. Merlino, M. Z. Shafikov, R. Czerwieniec, K. Kowalski, *Molecules* **2017**, *22*, 809-820.

[47] E. Hevia, J. Pérez, L. Riera, V. Riera, *Organometallics* **2002**, *21*, 1750-1752.

[48] E. Hevia, J. Pérez, L. Riera, V. Riera, I. del Río, S. García-Granda, D. Miguel, *Chem. Eur. J.* **2002**, *8*, 4510-4521.

[49] E. Hevia, J. Pérez, V. Riera, D. Miguel, *Organometallics* **2003**, *22*, 257-263.

[50] L. Cuesta, D. C. Gerbino, E. Hevia, D. Morales, M. E. Navarro-Clemente, J. Pérez, L. Riera, V. Riera, D. Miguel, I. del Río, S. García-Granda, *Chem. Eur. J.* **2004**, *10*, 1765-1777.

[51] L. Cuesta, E. Hevia, D. Morales, J. Pérez, V. Riera, E. Rodríguez, D. Miguel, *Chem. Commun.* **2005**, 116-117.

[52] L. Cuesta, E. Hevia, D. Morales, J. Pérez, V. Riera, M. Seitz, D. Miguel, *Organometallics* **2005**, *24*, 1772-1775.

[53] R. Arévalo, M. Espinal-Viguri, M. A. Huertos, J. Pérez, L. Riera, *Adv. Organomet. Chem.* **2016**, *65*, 47-114.

[54] F. Villafañe, *Coord. Chem. Rev.* **2017**, *339*, 128-137.

[55] M. T. Ashby, J. H. Enemark, *Organometallics* **1987**, *6*, 1323-1327.

[56] H. Adams, N. A. Bailey, A. N. Day, M. J. Morris, M. M. Harrison, *J. Organomet. Chem.* **1991**, *407*, 247-258.

[57] A. L. Serrano, M. A. Casado, M. A. Ciriano, B. de Bruin, J. A. López, C. Tejel, *Inorg. Chem.* **2016**, *55*, 828-839.

[58] A. Antiñolo, S. García-Yuste, I. Lopez-Solera, A. Otero, J.C. Pérez-Flores, R. Reguillo-Carmona, E. Villaseñor, E. Santos, E. Zuidema, C. Bo, *Dalton Trans.* **2010**, *39*, 1962-1971.

[59] C. Huang, H. Liu, J. Zhang, Z. Duan, F. Mathey, *Eur. J. Inorg. Chem.* **2010**, 5498-5502.

[60] D. A. M. Kurtz, K. R. Brereton, K. P. Ruoff, H. M. Tang, G. A. N. Felton, A. J. M. Miller, J. L. Dempsey, *Inorg. Chem.* **2018**, *57*, 5389-5399.

[61] D. Álvarez, R. Mera-Adasme, L. Riera, G. I. Cárdenas-Jirón, J. Pérez, J. Díaz, M. I. Menéndez, R. López, *Inorg. Chem.* **2017**, *56*, 6652-6661.

[62] (a) C. Gonzalez, H. B. Schlegel, *J. Chem. Phys.* **1989**, *90*, 2154-2161. (b) C. Gonzalez, H. B. Schlegel, *J. Phys. Chem.* **1990**, *94*, 5523-5527.

[63] (a) C. Riplinger, F. Neese, *J. Chem. Phys.* **2013**, *138*, 034106-18. (b) C. Riplinger, B. Sandhoefer, A. Hansen, F. Neese, *J. Chem. Phys.* **2013**, *139*, 134101-13.

[64] (a) F. Weigend, R. Ahlrichs, *Phys. Chem. Chem. Phys.* **2005**, *7*, 3297-3305. (b) D. Andrae, U. Haeussermann, M. Dolg, H. Stoll, H. Preuss, *Theor. Chim. Acta* **1990**, *77*, 123-141.

[65] (a) V. Barone, M. Cossi, *J. Phys. Chem. A* **1998**, *102*, 1995-2001. (b) J. L. Pascual-Ahuir, E. Silla, *J. Comput. Chem.* **1990**, *11*, 1047-1060. (c) J. L. Pascual-Ahuir, E. Silla, I. Tuñón, *J. Comput. Chem.* **1991**, *12*, 1077-1088. (d) J. L. Pascual-Ahuir, E. Silla, I. Tunón, *J. Comput. Chem.* **1994**, *15*, 1127-1138. (e) T. N. Truong, E. V. Stefanovich, C*hem. Phys. Lett.* **1995**, *240*, 253-260.

[66] T. J. Lee, P. R. Taylor, *Int. J. Quantum Chem.* **1989**, *36*, 199-207.

[67] D. G. Liakos, F. Neese, *J. Chem. Theory Comput.* **2015**, *11*, 4054-4063.

[68] D. A. McQuarrie, *Statistical Mechanics*, Harper and Row: New York, **1976**.

[69] R. F. Ribeiro, A. V. Marenich, C. J. Cramer, D. G. Truhlar, *J. Phys. Chem. B* **2011**, *115*, 14556-14562.

[70] (a) E. D. Glendening, A. E. Reed, J. E. Carpenter, F. Weinhold, NBO Version 3.1.; University of Wisconsin: Madison, WI, **2012**. (b) F. Weinhold, C.R. Landis, *Valency and Bonding: A Natural Bond Orbital Donor-Acceptor Perspective*; Cambridge University Press: Cambridge, **2005**.

[71] M. J. Frisch, G. W. Trucks, H. B. Schlegel, G. E. Scuseria, M. A. Robb, J. R. Cheeseman, G. Scalmani, V. Barone, B. Mennucci, G. A. Petersson, H. Nakatsuji, M. Caricato, X. Li, H. P. Hratchian, A. F. Izmaylov, J. Bloino, G. Zheng, J. L. Sonnenberg, M. Hada, M. Ehara, K. Toyota, R. Fukuda, J. Hasegawa, M. Ishida, T. Nakajima, Y. Honda, O. Kitao, H. Nakai, T. Vreven, J. A. Jr Montgomery, J. E. Peralta, F. Ogliaro, M. Bearpark, J. J. Heyd, E. Brothers, K. N. Kudin, V. N.

FULL PAPER

WILEY-VCH

Staroverov, R. Kobayashi, J. Normand, K. Raghavachari, A. Rendell, J. C. Burant, S. S. Iyengar, J. Tomasi, M. Cossi, N. Rega, J. M. Millam, M. Klene, J. E. Knox, J. B. Cross, V. Bakken, C. Adamo, J. Jaramillo, R. Gomperts, R. E. Stratmann, O. Yazyev, A. J. Austin, R. Cammi, C. Pomelli, J. W. Ochterski, R. L. Martin, K. Morokuma, V. G. Zakrzewski, G. A. Voth, P. Salvador, J. J. Dannenberg, S. Dapprich, A. D. Daniels, O. Farkas, J. B. Foresman, J. V. Ortiz, J. Cioslowski, D. J. Fox, Gaussian 09, Revision A.1, Gaussian, Inc., Wallingford CT, **2009**.

[72]   (a) X. Fradera, M. A. Austen, R. F. W. Bader, *J. Phys. Chem. A* **1999**, *103*, 304-314. (b) X. Fradera, J. Poater, S. Simon, M. Durán, M. Solá, *Theor. Chem. Acc.* **2002**, *108*, 214-224.

[73]   T. A. Keith, AIMAll program, Version 10.12.11, **2010**.

[74]   (a) R. F. W. Bader, A*toms in Molecules. A Quantum Theory*; University Press: Oxford, **1990**. (b) R. F. W. Bader, *Chem. Rev.* **1991**, *91*, 893-928.

[75]   F. Neese, Software Update: The ORCA Program System, Version 4.0.1, *WIREs Comput. Mol. Sci.* **2018**, *8*: e1327. DOI: 10.1002/wcms.1327.

Entry for the Table of Contents

FULL PAPER

Computations reveal that the YR ligand determines both the reaction pattern and the obtained product in the reaction between [Re(YR)(CO)$_3$(bipy)] complexes and activated alkynes. Since all patterns start with the same nucleophilic addition, the experimental selectivity is dictated by the kinetics and/or thermodynamics of the last stage of the reaction.
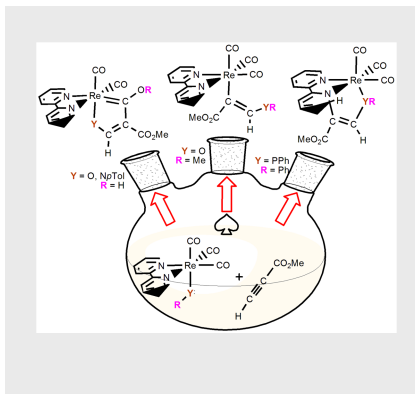
Coordination Chemistry

Daniel Álvarez, Jesús Díaz, M. Isabel Menéndez, Ramón López*

Page No. – Page No.

Addition of Re-Bonded Nucleophilic Ligands to Activated Alkynes: A Theoretical Rationalization